

# Orbital Monitoring of the Ionosphere and Abnormal Phenomena by the Small Vulkan-Compass-2 Satellite

V. D. Kuznetsov<sup>a</sup>, L. Bodnar<sup>b</sup>, G. K. Garipov<sup>c</sup>, V. A. Danilkin<sup>d</sup>, V. G. Degtyar<sup>d</sup>, V. S. Dokukin<sup>a</sup>, T. A. Ivanova<sup>†, e</sup>, O. V. Kapustina<sup>a</sup>, V. E. Korepanov<sup>e</sup>, Yu. M. Mikhailov<sup>a</sup>, N. N. Pavlov<sup>c</sup>, M. I. Panasuyk<sup>c</sup>, I. S. Prutenskii<sup>a</sup>, I. A. Rubinshtein<sup>c</sup>, Yu. Ya. Ruzhin<sup>a</sup>, V. M. Sinelnikov<sup>a</sup>, V. I. Tulupov<sup>c</sup>, Ch. Ferents<sup>b</sup>, A. V. Shirokov<sup>c</sup>, and I. V. Yashin<sup>c</sup>

<sup>a</sup> Pushkov Institute of Earth Magnetism, Ionosphere, and Radiowave Propagation (IZMIRAN), Russian Academy of Sciences, Troitsk, Moscow oblast, 142190 Russia

<sup>b</sup> Space Research Groupe Etwos University, Budapest, Hungary

<sup>c</sup> Lomonosov Moscow State University Skobeltsyn Institute of Nuclear Physics (MSU SINP), Moscow 119991, Russia

<sup>d</sup> Open Joint Stock Company “Academician V.P. Makeyev State Rocket Centre”, Miass 456300, Russia,

<sup>e</sup> Center of Cosmic Investigation of NANU and NCAU, Lvov, 79000 Ukraine

Received May 25, 2010; in final form, September 21, 2010

**Abstract**—Natural disasters, the processes of their origin and large-scale technogenic catastrophes are accompanied by anomalous physical phenomena in near-Earth space (NES). In order to reveal such phenomena, record and investigate them, complex NES monitoring is required with the use of specially designed research equipment onboard a low-orbiting spacecraft. This work presents the results of flight tests of the small Vulkan-Compass-2 satellite with research equipment specially designed for orbital monitoring of the ionosphere and search for abnormal phenomena caused by large-scale catastrophes of different nature.

**DOI:** 10.1134/S001679321103011X

## 1. INTRODUCTION

An urgent problem of near-Earth space (NES) orbital monitoring is the search for abnormal physical phenomena connected to both natural disasters, their background, and probable forerunners and the resulting technogenic catastrophes.

At present, a series of abnormal physical phenomena in the Earth’s lithosphere, atmosphere, ionosphere, and magnetosphere have been revealed and separated against the background of the known variations in NES parameters caused by interactions between the solar radiation and solar wind and the Earth’s magnetosphere, ionosphere, magnetic field, and surface; these phenomena originate from catastrophic events on the Earth, including earthquakes, tropical cyclones, tornados, nuclear tests, accidents at nuclear plants, etc. (Liperovskii et al., 1992; Oraevskii et al., 1994; Oraevskii et al., 1995; Ruzhin and Depueva, 1996; Bychachanko et al., 1996; Ruzhin and Larkina, 1996; Fuks and Shubova, 1994; Ruzhin et al., 1995; Isaev et al., 2002; Sorokin et al., 2005; Oraevskii et al., 1995; Calais and Minster, 1996; Nagorskii, 1998; Afraimovich et al., 2002; Rapoport et al., 2004; Ruzhin and Depueva, 1995; Dokukin et al., 2000; Ruzhin and Kuznetsov, 2005). Physical models and mechanisms, which allow for the explanation of some

features of the revealed phenomena, have been actively and successfully discussed in the last years, though no general clarity has been achieved.

Variations in NES parameters associated with seismic activity at the early phase of powerful earthquakes are of special interest. The available records show that investigations in this direction are promising for further design of a practical system for NES monitoring and diagnostics of earthquake forerunners. However, the records lack any regular pattern, and the use of data archives and bases is mainly retrospective. Further progress in these researches is only possible due to target programs of NES monitoring, design of a specially purposed complex of research equipment and corresponding software.

The project Vulkan-Compass-2 was worked out and implemented in 2006–2007 on the initiative of IZMIRAN within the Russian Federal space program; it included the design of a new space platform, i.e., the small Vulkan-Compass-2 spacecraft and a specially purposed complex of research equipment for ionospheric monitoring and search for abnormal physical phenomena connected to natural and technogenic catastrophes, including forerunners of large earthquakes.

The main goal of the Vulkan-Compass-2 satellite launching was flight tests and the working out of the main components of the system for the purposes of

<sup>†</sup> Deceased.

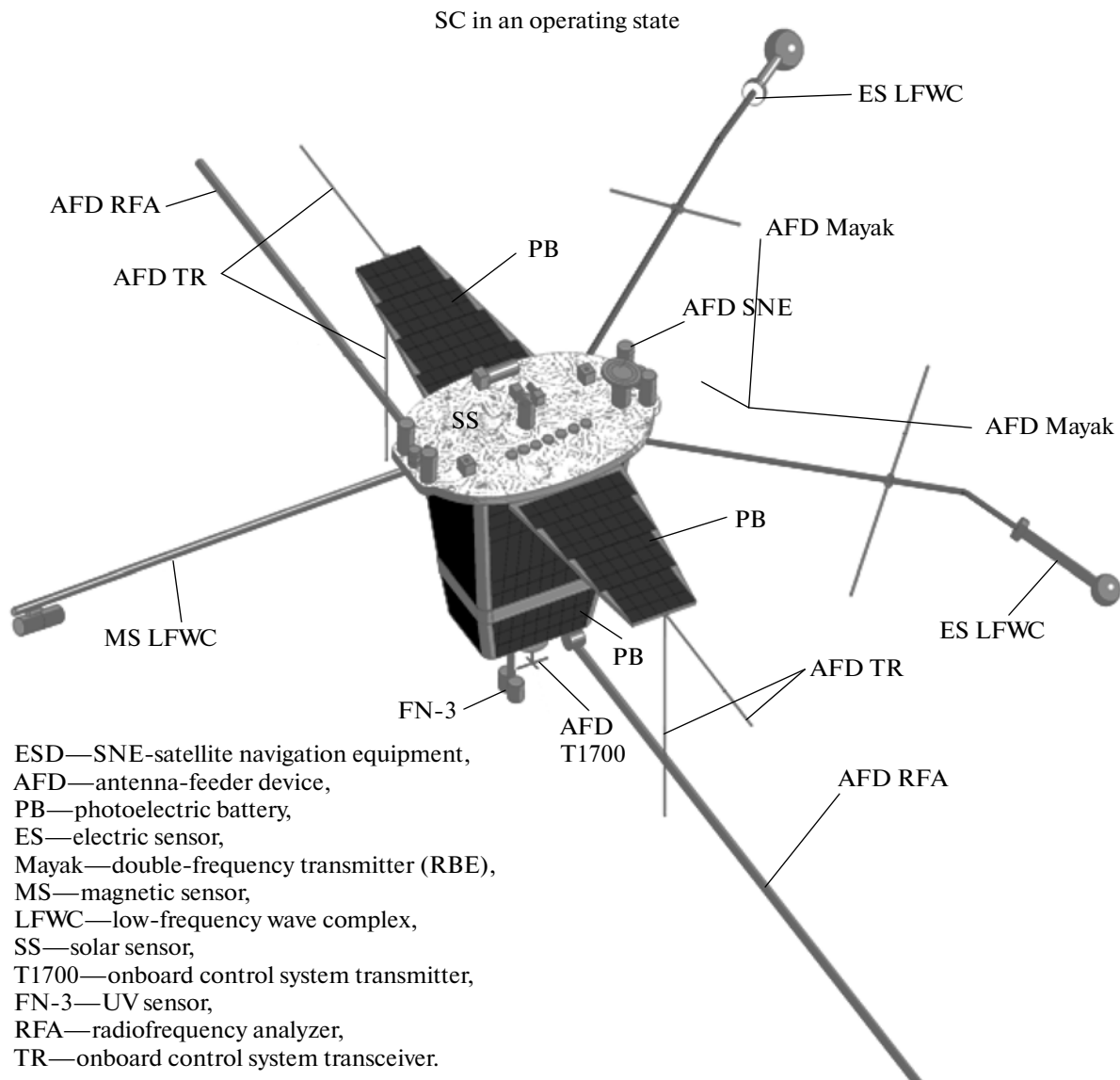


**Fig. 1.** General configuration of the Vulkan-Compass-2 SSC.

designing a natural and technogenic catastrophe monitoring space system.

## 2. SMALL VULKAN-COMPASS-2 SPACECRAFT (SSC)

The experimental Vulkan-Compass-2 SSC (Fig. 1) was launched to the near-earth orbit with an inclination of  $78.90^\circ$ , apogee of 519.0 km, perigee of 412.3 km, and a revolution period of 93.59 min on May 26, 2006. The total mass of the SSC was 80 kg (including 20 kg of research equipment).

During this pilot project, specially designed research equipment should be tested, its operation

regimes and specifications, a technique for on-line data acquisition, processing, and analysis, and new support systems of the microsatellite: a central on-board processor; radio-channel device for telemetry and radiocontrol; and orientation, thermocontrol and power supply systems.

The project was implemented with the participation of the Academician V. P. Makeyev State Rocket Centre on the part of the rocket and space complex (satellite platform Compass-2 (Fig. 1), converted missile PCM-54 (Shtil), and support of the SC launch from a submarine in the Barents Sea), IZMIRAN on the part of scientific-methodological project development and supply of on-board research equipment, the

Main specifications of the Compass-2 complex of research equipment

No.	Instrument	Weight, kg	Consumption, W	Dataflow, Mb/day	Measurement range
1	Radiofrequency analyzer (RFA)	1.8	3.4	21	50 kHz÷18 MHz
2	Low-frequency wave analyzer ELF/VLF	3	5	50	0.1 Hz÷20 kHz
3	Dual-frequency transmitter 150/400 Mayak	2	6	0	150/400 MHz
4	Dual-frequency GPS receiver of the satellite navigation equipment (SNE)	2	3	25	1.2 GHz/1.5 GHz
5	Radiation and ultraviolet detector (DRF)	4.5	3	4	$E_a \geq 40 \text{ keV}; 300\text{--}600 \text{ keV};$ $\geq 0.7\text{--}0.9 \text{ MeV}$ $E_p \geq 7\text{--}16 \text{ MeV}; 14\text{--}60 \text{ MeV};$ $\geq 110 \text{ MeV}$ $E_\alpha \geq 400 \text{ MeV}$ $\lambda = 200\text{--}350 \text{ nm}$

Scobeltsyn Nuclear Physics Institute (Moscow State University), and international cooperation (Ukraine, Hungary, Poland, and Sweden).

MCC TSNIIMASH (Korolev city), movable and stationary MCCs of the Academician V. P. Makeyev State Rocket Centre (Miass) and IZMIRAN (Troitsk) controlled the COMPASS-2 satellite.

### 3. COMPLEX OF RESEARCH EQUIPMENT

The complex of research equipment of the Vulkan-Compass-2 SSC included five scientific instruments for measuring altitude profiles and variations in ionospheric parameters and electromagnetic radiation, as well as variations in the parameters and fluxes of energetic particles.

The ionospheric complex included the following instruments:

(1) a dual-frequency (1.2 and 1.5 GHz) GPS receiver of the satellite navigation equipment (SNE) for global monitoring of the atmosphere and ionosphere by the radio occultation method;

(2) a dual-frequency transmitter RBE 150/400 Mayak for the radiotomographic reconstruction of the ionosphere and its local anomalies.

Receiver-analyzers of electromagnetic radiation were as follows:

(1) a radiofrequency analyzer RFA (from 50 kHz to 18 MHz) for recording plasma radiation in the iono-

sphere, which allows for the determination of basic plasma parameters near the SC, including the local plasma frequency at the satellite altitude;

(2) a low-frequency wave analyzer ELF/VLF in the 0.1–20 kHz frequency range for recording and analyzing abnormal low-frequency noises connected to seismic activity in NES.

Finally, the complex included a radiation and UV detector DRF for recording the electrons and protons of the Earth's radiation belts and cosmic rays, as well as UV radiation in the Earth's upper atmosphere.

The specifications of the complex instruments are given in the table.

### 4. SCIENTIFIC RESULTS

The problems and limitations of the trial operations of the platform of the Compass-2 CCS connected to the abnormal functioning of its support systems, i.e., the radiocontrol channel and power supply system, were revealed during flight tests.

Despite these limitations, the main tasks of trying out of the CCS research complex instruments were successfully solved during the flight tests.

The main specifications of the instruments were verified and confirmed. Several cycles of NES parameter measurements and monitoring were performed over seismoactive regions. Measurement data were received on the ionospheric background conditions; phenomena of strong thunderstorm activity in the

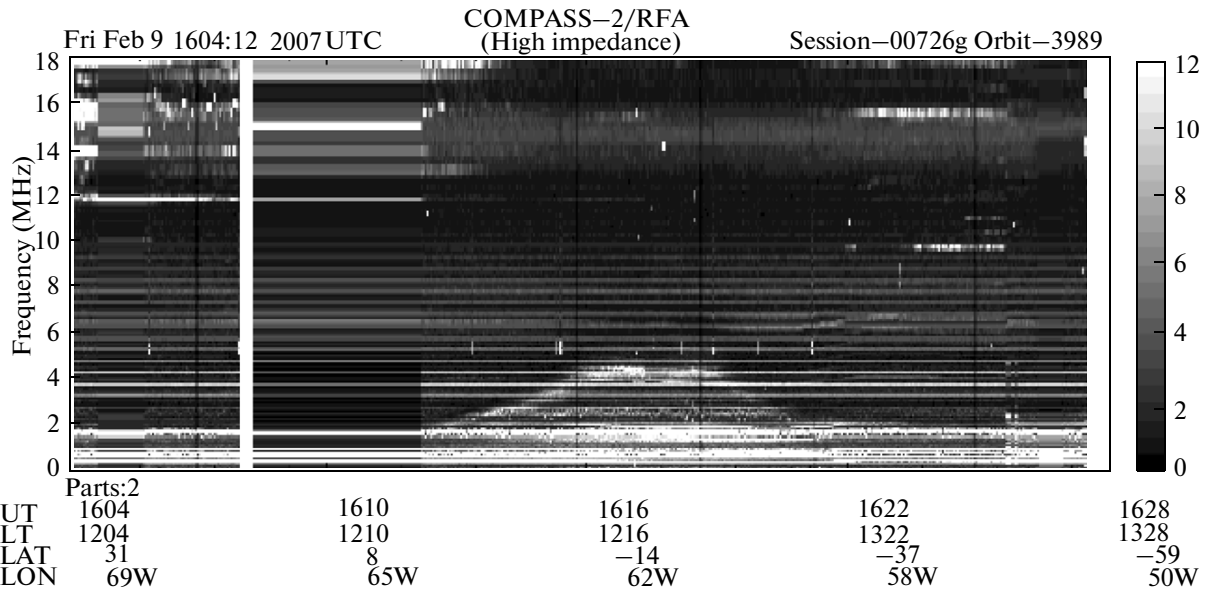


**Fig. 2.** Dynamic spectrum recorded by an RFA while flying over the equatorial anomaly region on February 9, 2007, at high antenna-feed impedance. The frequency range of the instrument is shown on the left, the palette of the received signal intensity in TM units is shown on the right, and orbital data (universal time, local time, latitude, and west longitude) are given at the bottom.

upper atmosphere were recorded; fluxes of accelerated protons and electrons connected to the solar activity during a large geomagnetic storm on December 15, 2006, were recorded in NES; SSC was positioned with the use of SNE for GPS signals; the actual possibility of using SNE in calculations of CS orbital data and highly-accurate timing of measurement data was demonstrated during unique synchronous experiments with ground-based and orbital tools in a unified time system; and whistlers, their short passage from the Earth's surface to the satellite (partially dispersed whistlers), ELW station line broadening and whistler signals accompanying seismoactive processes were registered.

Figure 2 exemplifies the dynamic spectrum recorded by RFA while flying over the equatorial anomaly region on February 9, 2007, with high antenna feed impedance.

Energetic particles and atmospheric glows of different nature were recorded by DRF. The DRF measurements allowed for the controlling of the geophysical situation in the satellite's orbit, which is very important for interpreting data and distinguishing between background and abnormal events.

The measurement results of energetic particle fluxes are exemplified in Figs. 3–5; the measurements were carried out at night from December 14 to 15, 2006. This period was full of events in the Earth's magnetosphere and interplanetary space (Tverskaya et al., 2008). A drop in the intensity of proton components injected into interplanetary space by a burst on

December 13 was observed in solar cosmic rays (SCR). After that, particles originated from a new solar burst at 2214 UT on December 14 arrived to the Earth. The passage of a high-speed coronal mass ejection (CME) through the Earth's orbit was recorded in the solar wind from 1414 to 2300 UT on December 14. The beginning of a magnetic storm was recorded in the geomagnetic situation at about 2300 UT with the maximum  $|Dst| = 146$  nT attained at 0800 UT on December 15.

Figure 3 shows the population of the polar cap with SCR protons with  $Ep = 7\text{--}15$  MeV (plateau-like increases); an increase in proton fluxes with  $Ep = 15\text{--}40$  MeV while passing the cap at 0040–0100 UT; increases connected to the South Atlantic magnetic anomaly (growths to the left of the plateau observed in the South hemisphere). Figure 4 allows one to see the geographical localization of the South Atlantic Anomaly (the gas discharge channel added in Fig. 4 is used for its indication). Figure 5 shows measurement data on energetic electron fluxes; it is possible to see the South Atlantic Anomaly, radiation belts, polar cap (due to SCR protons with  $Ep > 7$  MeV in channel I), variations of different scales in fluxes in both caps and belts, North–South and day–night asymmetries, decrease in the latitude of the auroral zone, population of a region near the inner belt with electrons of  $Ee = 300\text{--}600$  keV with their shift deep into the magnetosphere on the dayside during the period near the local minimum  $Dst$ .

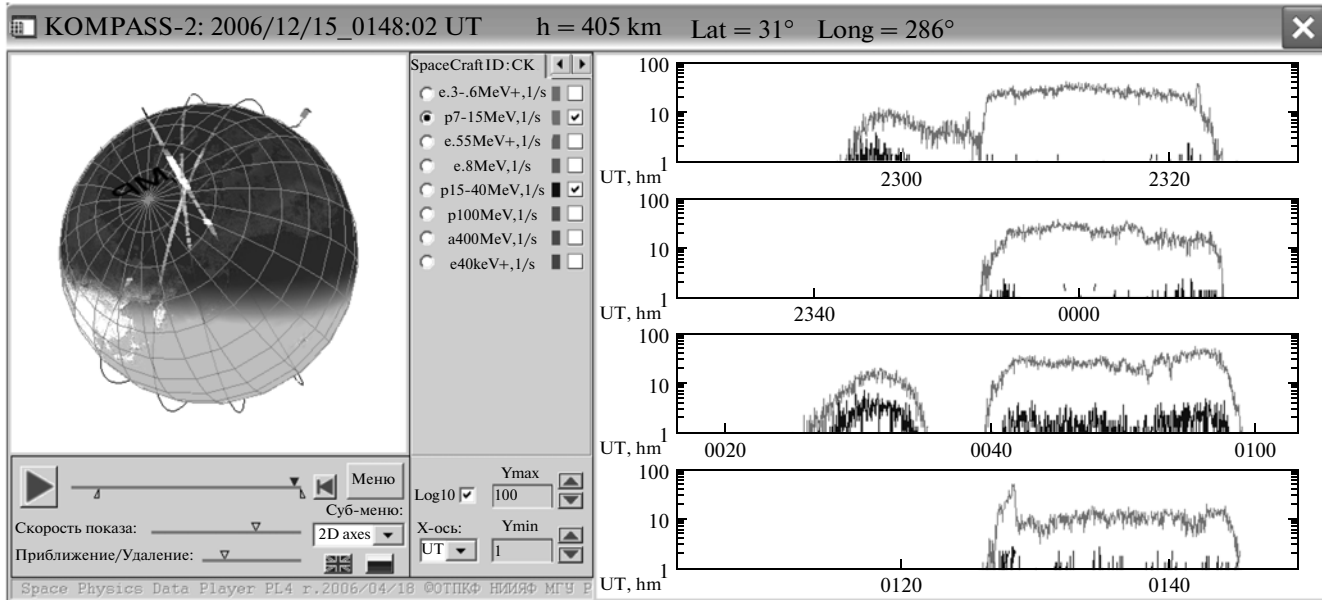


**Fig. 3.** DRF data on proton fluxes in the period from 2245 UT on December 14 to 0148 UT on December 15, 2006. The right part shows the time behavior of the counting rate of 7–15 MeV (light grey curve) and 15–40 MeV (dark curve) protons when flying over the southern (the first and third panels) and northern (the second and fourth panels) hemispheres. The left part shows the northern polar cap of the Earth with satellite lightning by data from the 7–15 MeV proton channel (the lighter and heavier the curve, the higher the counting rate is) and indication of the magnetic pole (MP) position.

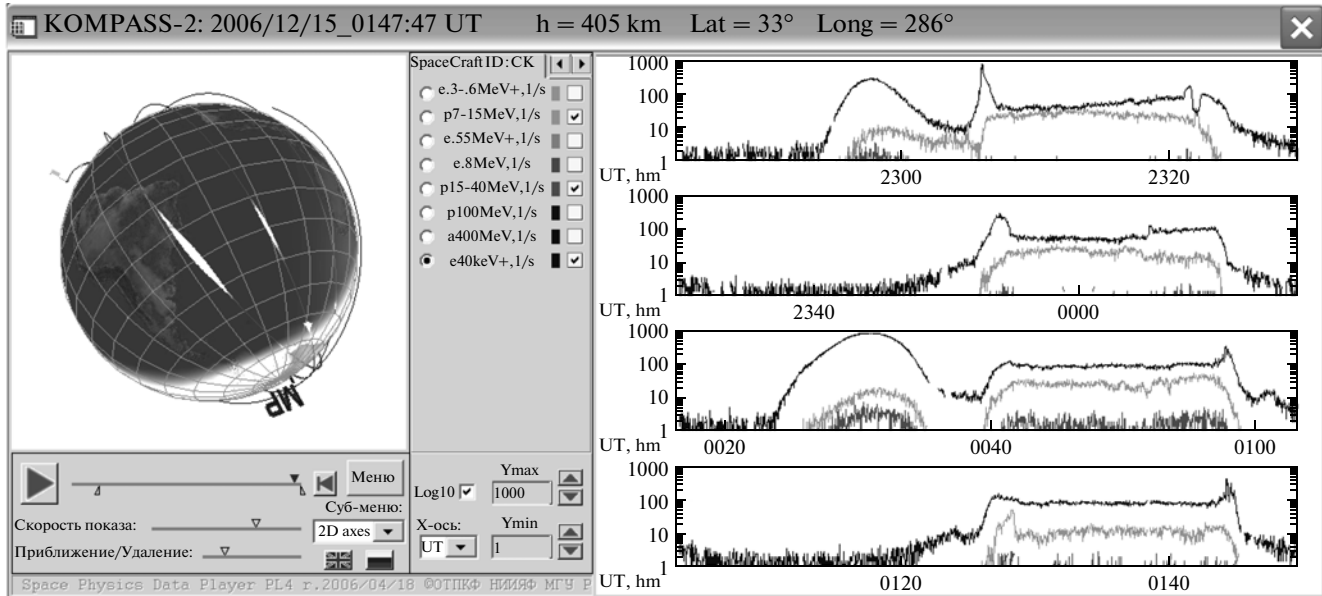


**Fig. 4.** The same as in Fig. 3, but a gas-discharge counter channel is added in the right part (the darkest curve), and the satellite passage over the South Atlantic Anomaly is shown in the data of this counter in the left part.

Figures 6–7 show oscilloscopes recorded on the nightside of the Earth with the use of the DRF detector.

The records of low-frequency electromagnetic signals by the low-frequency wave analyzer ELF/VLF are the most informative and interesting (Likhite et al., 1988; Mikhailov et al., 2004; Dowden et al., 2004; Ferencz et al., 2008, 2009; Lichtenberger et al.,

2009; Mikhailov et al., 2008). A lot of attention was paid to the study of different types of whistlers.

The following phenomena were recorded during the observations:

**Partially dispersed whistlers over Indonesia.** The spectrogram in Fig. 8 shows the paths of discrete sig-

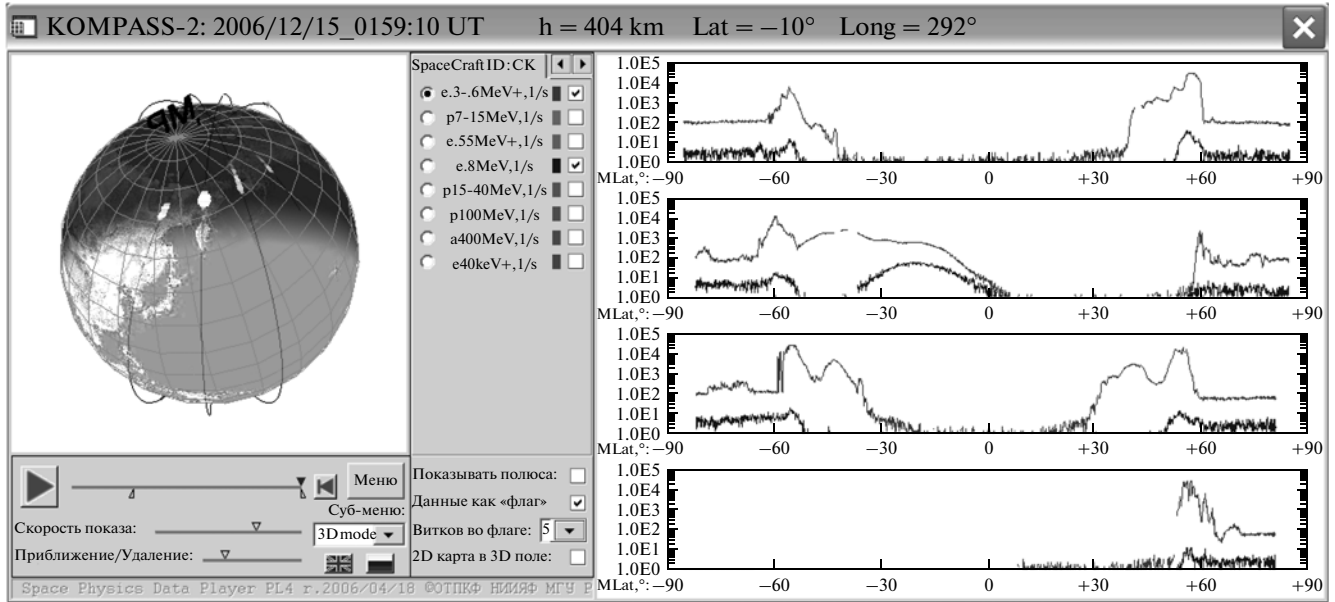


**Fig. 5.** DRF data from electron detectors for the same period as in Figs. 3 and 4. The right part shows the counting rate with threshold energies (1)  $E_e = 300\text{--}600 \text{ MeV}$  +  $E_p > 7 \text{ MeV}$  (light gray curve) and (4)  $E_p > 7 \text{ keV}$  (dark curve); the magnetic latitude is given along the  $X$ -axis. The left part shows the north polar cap of the Earth with satellite orbit lightning by the data channel (1).

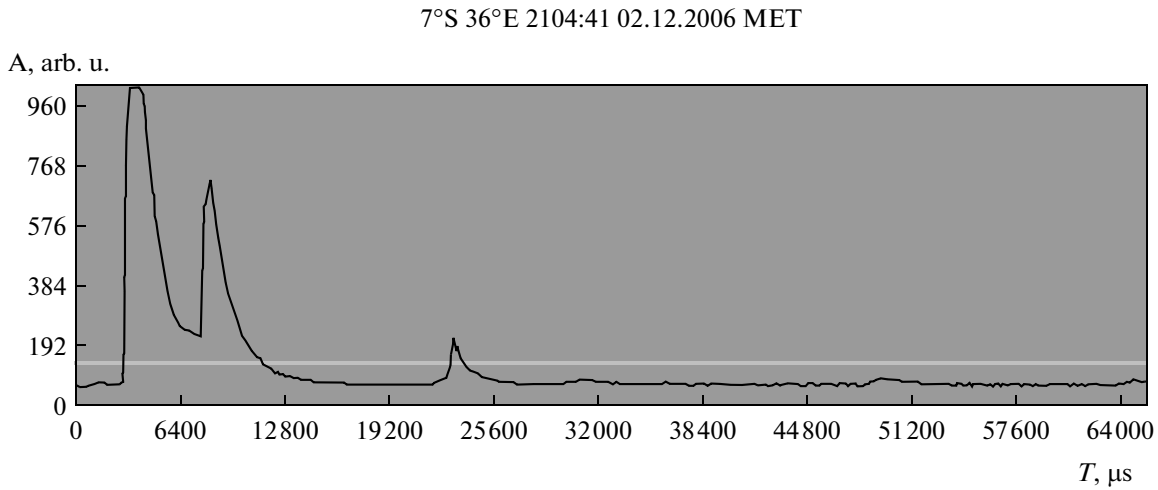


**Fig. 6.** Oscillogram shows a strong thunderstorm phenomena over Kenya recorded by a UV sensor on the nightside of the Earth at 2104:41 UT on December 2, 2006. The initial double pulse seemingly corresponds to two almost synchronous discharges.

nals, the frequency of which smoothly decreased over time. These are partially dispersed whistlers generated by lightning discharges and propagating along the short path from the Earth–ionosphere waveguide to the satellite altitudes. The top fragment shows a spectrogram of the electric component and the bottom one shows that of the magnetic component. The intensity scale is depicted on the left. The analysis of the lightning discharge distribution at 0500:00 UT on November

29, 2006, (Dowden et al., 2004) has shown the presence of a large number of lightnings in Indonesia's zone. For partially dispersed whistlers, the variance  $Dst$  is about 5, and the spectrum maximum has a frequency of 2500 Hz.

**Whistler doublets.** Whistler doublets (or whistler pairs) have been observed from satellites for a long time; however, much remains to be studied about their propagation. Figure 9 shows the measurement results of

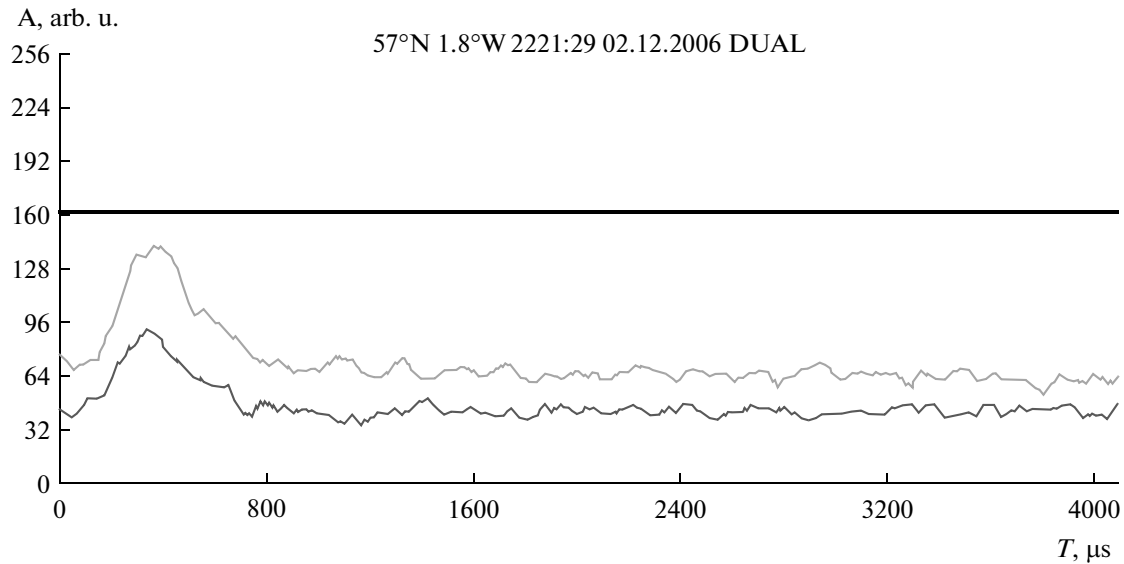


**Fig. 7.** Radiation oscillograms recorded by the DRF UV sensor on the nightside of the Earth at 2221:29 UT on December 2, 2006: measurements in UV channels (light gray curve) and red wavelength range (dark curve) (rapid optical phenomenon recorded over Scotland).

whistler doublets by the Intercosmoc-24 (on the left) and Compass-2 (on the right) satellites. The occurrence of doublets at small altitudes points to the possibility of their origination during propagating along close ducts; at the same time, the probability of their origination due to reflections from the ionosphere is low.

**Multipath branching whistlers.** One of the interesting results received by the Vulkan-Compass-2 satellite is the detection of an unusual frequency dependence of multipath branching whistlers within the 0–100 Hz range. At the satellite, this spectral region was free of interferences, which allows the tracing of the frequency–time dependence  $f(t)$  with a high accuracy. The  $t \rightarrow \infty$  curve is usually considered as asymptotically tending to but not reaching zero at  $f(t)$ . However, a possibility of propagation of high-order modes in ducts was recently assumed in the works of the Space Research Group, Eötvös University, Budapest, Hungary (Ferencz et al., 2009). This assumption was confirmed by whistler propagation calculations with accounting for the two-way wave equation. Magnetized plasma was considered where the electron density distribution forms a concentric waveguide around the  $H_x$  component of the magnetic field; the propagation of modes of higher orders (bulbous structure) is possible in this waveguide. Figure 10 shows a model representation of the frequency–time characteristics of the electric and magnetic components of a whistler propagating in a similar structure in the form of a third-order mode. The parameters of the above-mentioned components of a whistler registered on the SSC on February 28, 2007, are also given in Fig. 10,

although the spatial orientation of these components was not identified. As is seen in Fig. 10, the  $f(t)$  characteristic reaches zero during a finite time interval. This allows for an assumption about the propagation of a whistler in the form of a third-order mode in a concentric waveguide. Unfortunately, the observations on the Vulkan-Compass-2 SSC were insufficient for a complete statistical pattern of the phenomenon, which will be addressed in future experiments.

**Noise storm burst over Central Europe.** While flying over Central Europe, an unusual high-level signal in a narrow frequency range of 500–2000 Hz was observed in a sonogram recorded by the satellite (Fig. 11). It was similar to a low-frequency partially-dispersed whistler with a follow-up noise emission at the maximum frequency in the partially-dispersed whistler spectrum or it was a series of almost indivisible partially-dispersed whistlers. The TOGA system (Dowden et al., 2002) localized several whistlers in the Mediterranean at the same time.

**Broadening of ELW transmitter signals.** When monochromatic waves interact with magnetosphere plasma, trigger emissions or broadening of the frequency spectrum of signals occur (Fig. 12).

Trigger emissions are seemingly connected to resonance interactions between ELF waves and electrons in radiation belts in the inhomogeneous magnetic field. The frequency spectrum broadening effects can be caused by magnetospheric interactions between whistler waves and particles.

**Signals in seismoactive regions.** The problem of propagation of strong electromagnetic signals through

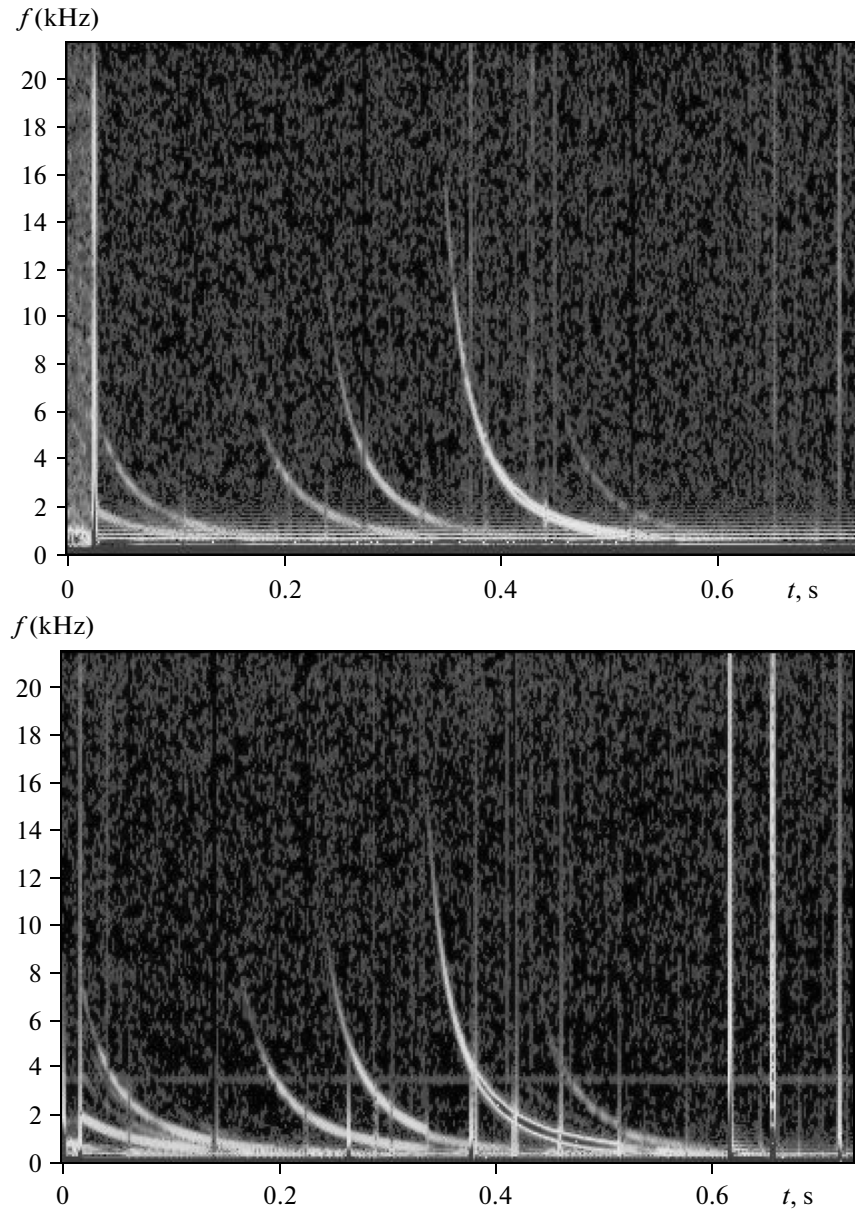


**Fig. 8.** Partially-dispersed whistlers recorded over Indonesia.

the lower ionosphere is quite urgent today. In view of this, we made an attempt to consider the propagation of signals of strong whistlers, which can be forerunners of earthquakes. Figure 13 shows the dynamic spectrum of low-frequency ELF/VLF radiation received while flying over Kamchatka at 2135:49 on February 27, 2007 (see Fig. 14). The recorded abnormal signals ( $A$  in the left part of Fig. 13) can be connected to the origination of an earthquake, which took place in the Kamchatka region on February 28, 2007, and had a magnitude of 4.2 (Fig. 14). A partially dispersed whistler with a spectral maximum at about 5 Hz is well seen in the first part of the frame, which indicates the possible arrival of a

whistler to the satellite from about 1000–1500 km. Figure 13 also shows a series of whistler traces ( $A$  in the right part); we succeeded to assess the variance in one of them ( $D \sim 72$ ). The region in the opposite hemisphere, from which the signals could have arrived to the satellite along geomagnetic lines of force, can be estimated as well. The TOGA system localized a group of signals in the southeast part of Australia.

The light circle in the right upper corner of the map in Fig. 14 corresponds to the earthquake of class  $K = 11$  ( $M \sim 4.5$ ), while the black square corresponds to the satellite position at the time of recording.

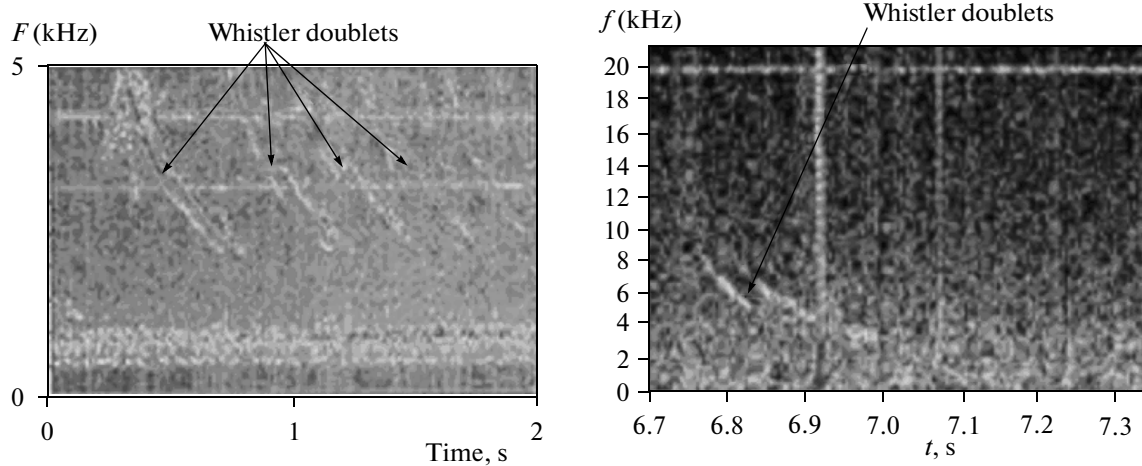


**Fig. 9.** Whistler doublets recorded by Intercosmos-24 (left) on December 14, 1990, and Compass-2 (right) on January 27, 2007.

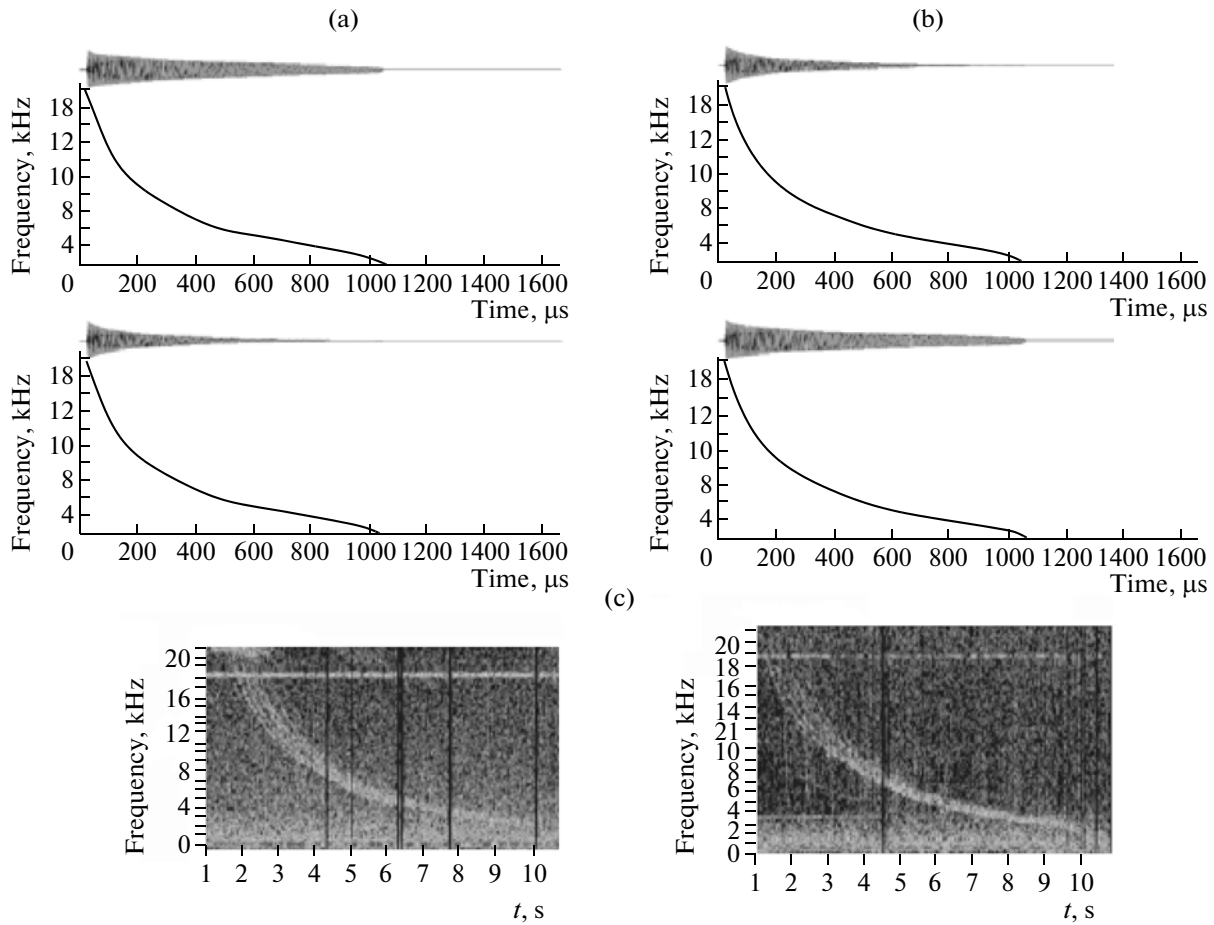


**Fig. 10.** Comparison of the model frequency–time characteristics of whistlers propagating in magnetized plasma in the form of a third-order mode with experimental results: model calculations of (a)  $E_y$  (top) and  $E_z$  (bottom), (b)  $H_y$  (top) and  $H_z$  (bottom), and (c) electric (left) and magnetic (right) components recorded by the Vulkan-Compass-2 satellite on February 28, 2007.

The ground-based data from the Paratunka observatory showed that sufficiently powerful radiation from the southwest direction and a small number of

whistlers arriving from other directions were observed while flying over Kamchatka at 2135:49 on February 27, 2007. A decrease in the signal level was noted at all

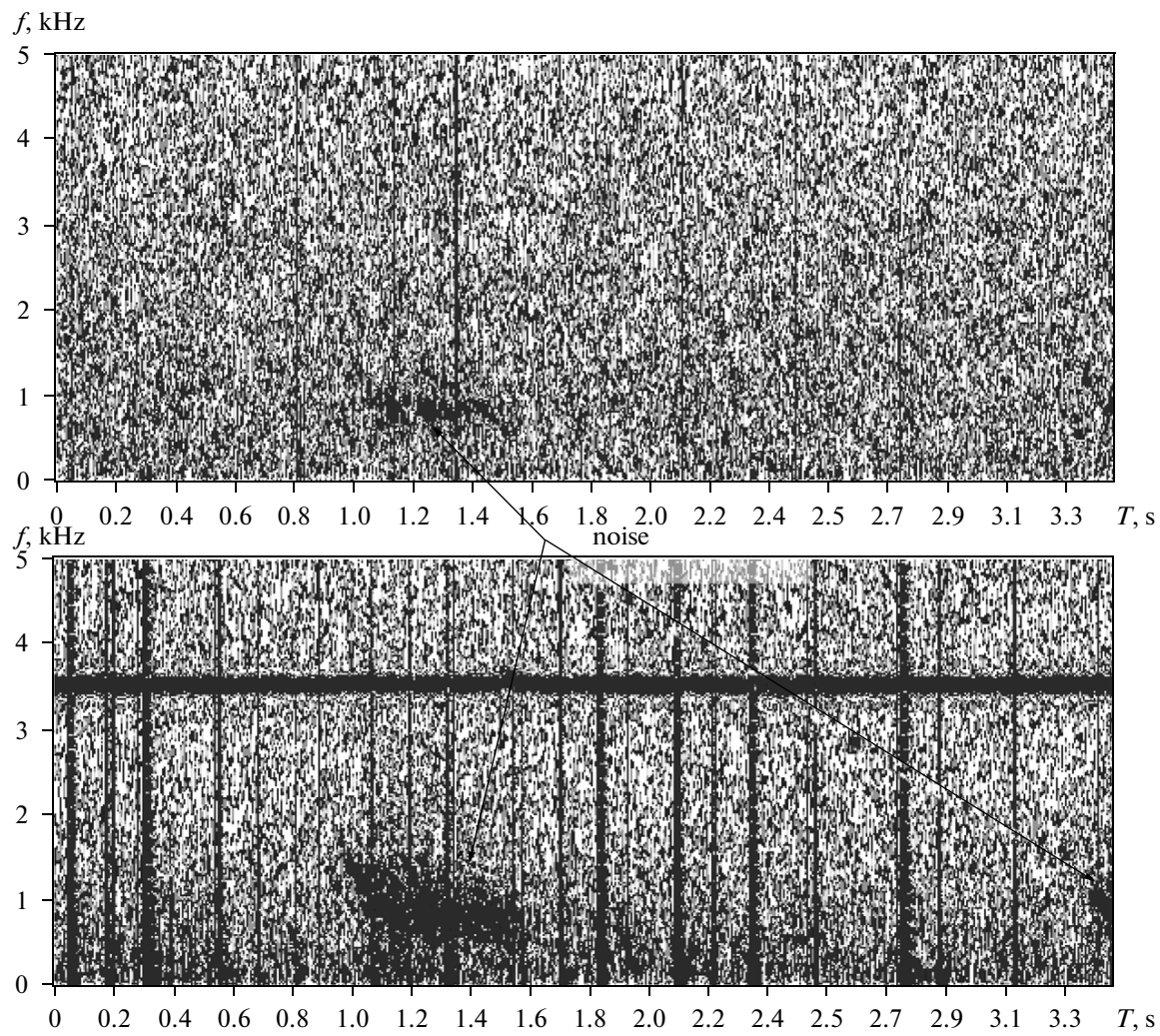


**Fig. 11.** Low-frequency noises probably connected to the particle precipitation recorded by an ELF analyzer over Central Europe at about 1002 UP on February 11, 2007. Zero on the time axis corresponds to the beginning of event.

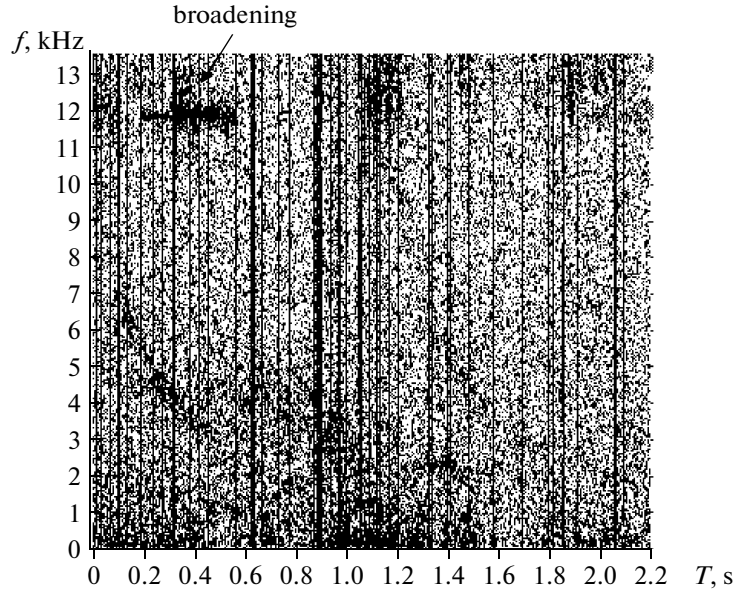


**Fig. 12.** Broadening of the frequency range of the transmitter signal at 1709:17 UT on March 18, 2007 (the electric component). Zero on the time axis corresponds to the beginning of event.

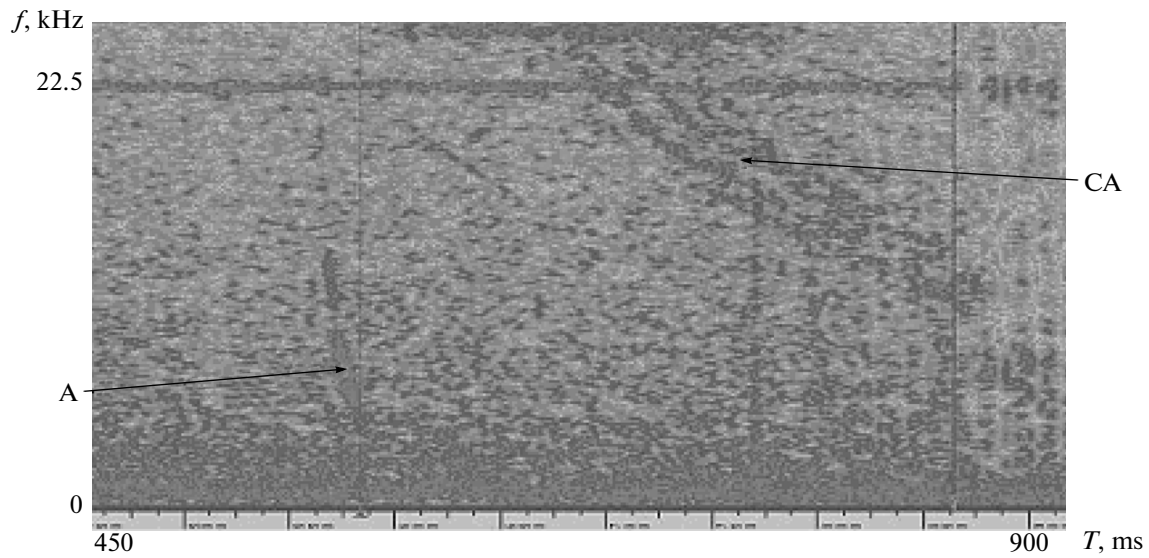


**Fig. 13.** Dynamic spectrum of the ELF recording received by the Vulkan-Comass-2 satellite while flying over Kamchatka (see Fig. 14).

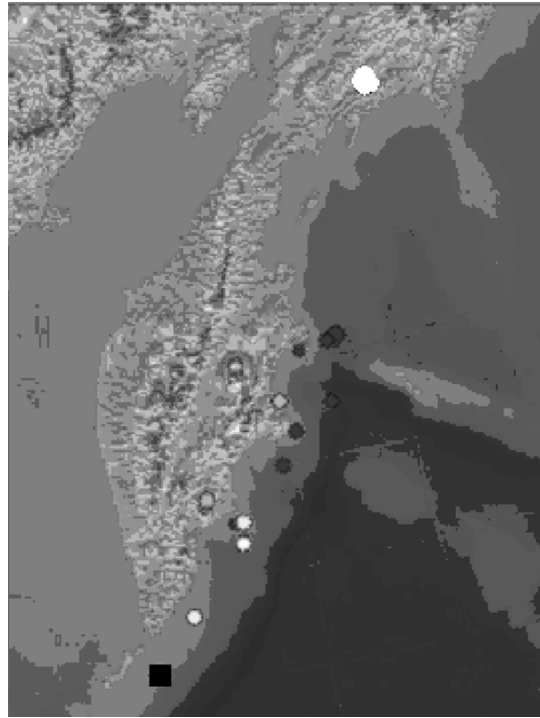


**Fig. 14.** Earthquake distribution over Kamchatka on February 2, 2007. The light circle in the upper right corner of the map corresponds to the earthquake of class  $K = 11$  ( $M \sim 4.5$ ), while the black square corresponds to the satellite position at the time of recording at 2135:49.

recording frequencies in the analogous recording on February 27, 2007, when the satellite was flying over Kamchatka at 2135:49; the radiation maximum was observed at 1900–2000 hours. The loop–antenna plane was positioned east–westward.

## 5. CONCLUSIONS

Flight tests and trial operation of the Vulkan-Comass-2 SSC complex of research equipment allowed for the measuring of the background state of the ionosphere; recording of strong thunderstorm activity in

the upper atmosphere, fluxes of accelerated protons and electrons in NES connected to solar activity during a large geomagnetic storm on December 15, 2006; SSC positioning with the use of an SNE device by GPS signals; demonstration of the practical usability of the SNE device for calculating SSC orbital data and highly-accurate timing of measurement data during unique synchronous experiments with the use of ground-based and orbital tools in a unified time system; recording of ELV-station spectrum broadening, whistlers, and the level of their signals accompanying seismoactive processes.

The trial operation of the Vulkan-Compass-2 SSC complex of research equipment showed that it can be used as a basis for scientific complexes of ionospheric monitoring in following projects and systems purposed for revealing and recording abnormal phenomena in NES connected to earthquakes and other natural and technogenic catastrophes. The software used for measurements and analyses of scientific instrument data was worked out during flight tests. The analysis of engineering problems and failures of the support systems of the microsatellite made it possible to find out their reasons and avoid them in further modifications of the Compass platform.

## REFERENCES

- Afraimovich, E.L., Perevalova, N.P., and Plotnikov, A.P., Registration of Ionospheric Responses to Shock Acoustic Waves Generated by Carrier Rocket Launches, *Geomagn. Aeron.*, 2002, vol. 42, no. 6, pp. 790–797 [*Geomagn. Aeron.*, (Engl. Transl.), 2002, vol. 42, pp. 755–762].
- Buchachenko, A.L., Oraevsky, V.N., Pokhotelov, O.A., Strakhov, V.N., Sorokin, V.M., and Chmyrev, V.M., Ionospheric Precursors of Earthquakes, *Usp. Fiz. Nauk*, 1996, vol. 166, no. 9, pp. 1023–1029.
- Calais, E. and Minster, J.B., GPS Detection of Ionospheric Perturbations Following a Space Shuttle Ascent, *Geophys. Res. Lett.*, 1996, vol. 23, pp. 1897–1900.
- Dokukin, V.S., Oraevsky, V.N., Alekseev, A.V., Velichko, I.I., Nikulin, Yu., and Sleta, A.V., The General Conception of the Microsatellite Compass to Be Launched from Submarine to Study of the Earthquakes Forerunners, *Acta Astronaut.*, 2000, vol. 46, no. 2–6, pp. 351–354.
- Dowden, R.L., Brundell, J.B., and Rodger, C.J., VLF Lightning Location by Time of Group Arrival (TOGA) at Multiple Sites, *J. Atmos. Sol.–Terr. Phys.*, 2002, vol. 64, pp. 817–830.
- Ferencz, O.E., et al., Guided Transient Signals in Space Plasmas, *Proc. 3rd VERSIM Workshop 2008*, J. Lichtenberger, Cs. Ferencz, and P. Steinbach., Eds., Tihany, 2008.
- Ferencz, O.E., Bodnar, L., Ferencz, C., Hamar, D., Lichtenberger, J., Steinbach, P., Korepanov, V., Mikhailova, G., Mikhailov, Yu., and Kuznetsov, V., Ducted Whistlers Propagating in Higher Order Guided Mode and Recorded on Board of COMPASS-2 Satellite by the Advanced Signal Analyzer and Sampler SAS2, *J. Geophys. Res.*, 2009, vol. 114, p. A03213; doi:10.1029/2008JA013542.
- Fuks, I.M. and Shubova, R.S., Anomalies in ULF Signals as a Response to the Processes in the Near-Earth Atmosphere, *Geomagn. Aeron.*, 1994, vol. 34, no. 1, pp. 130–134.
- Isaev, N.V., Sorokin, V.M., Chmyrev, V.M., and Serebryakova, O.N., Ionospheric Electric Fields Related to Sea Storms and Typhoons, *Geomagn. Aeron.*, 2002, vol. 42, no. 5, p. 670 [*Geomagn. Aeron.* (Engl. Transl.), 2002, vol. 42, p. 638–643].
- Lichtenberger, J., Ferencz, U.L., Bodnar, L., Hamar, D., and Steibach, P., Automatic Whistler Detector and Analyzer System: Automatic Whistler Detector, *J. Geophys. Res.*, 2009, vol. 113, p. A12201. doi: 10.1029/2008JA013467
- Likhter, Ya.I., Guglielmi, A.V., Erukhimov, L.M., and Mikhailova, G.A., *Volnovaya diagnostika prizemnoi plazmy* (Wave Diagnosis of the Near-Earth Plasma), Moscow.
- Liperovskii, V.A., Pokhotelov, O.A., and Shalimov, S.L., *Ionosfernye predvestniki zemletryasenii* (Ionospheric Precursors of Earthquakes), Moscow: Nauka, 1992.
- Mikhailov, Yu.M., Ferents, Sh., Lichtenberger, Ya., Bodnar, L., and Korepanov, V., Measuring ULF–VLF Electromagnetic Fields in the “COMPASS-2” Space Experiment, *Tez. dokl. na III mezhdunarodnoi konferentsii Solnechno-zemnye svyazi i elektromagnitnye predvestniki zemletryasenii*, (Proc. 3rd Int. Conf. on Solar-Terrestrial Coupling and Electromagnetic Precursors of Earthquakes), Petropavlovsk-Kamchatski, 2004, p. 43.
- Mikhailov, Yu.M., Mikhailova, G.A., Kapustina, O.V., Druzhin, G.I., Smirnov, S.E., Ferencz, C.H., Lichtenberger, Ja., Bodnar, L., and Korepanov, V.E., COMPASS 2 Satellite and Ground Base VLF-Experiments, *Proc. AIS-2008 “Atmosphere, Ionosphere, Safety”*, Kaliningrad, 2008, p. 31.
- Nagorskii, P.M., Rocket-Produced Irregularity in the Ionospheric F-Region, *Geomagn. Aeron.*, 1998, vol. 38, no. 2, pp. 100–106 [*Geomagn. Aeron.* (Engl. Transl.), 1998, vol. 38, pp. 212–216].
- Oraevsky, V.N., Ruzhin, Yu., and Depueva, A.Kh., Seismoionospheric Precursors and Atmospheric Electricity, *Turk. J. Phys.*, 1994, vol. 18, no. 11, pp. 1229–1234.
- Oraevsky, V.N., Ruzhin, Yu., and Depueva, A.Kh., Anomalous Global Plasma Structures as Seismo Ionospheric Precursors, *Adv. Space Res.*, 1995a, vol. 15, no. 11, pp. (11)127–(11)130.
- Oraevsky, V.N., Ruzhin, Yu., Depueva, A.Kh., Kozlov, E.F., and Samorokin, N.I., The Subauroral Events Generated by Rocket Launching, *Adv. Space Res.*, 1995b, vol. 15, no. 11, pp. (11)153–(11)156.
- Rapoport, Y., Grimalsky, V., Hayakawa, M., Ivchenko, V., Juarez, R.D., Koshevaya, S., and Gotynyan, O., Change of Ionospheric Plasma Parameters under the Influence of Electric Field Which Has Lithosphere’s Origin and Due to Radon Emanation, *Phys. Chem. Earth*, 2004, vol. 29, pp. 579–587.
- Ruzhin, Yu. and Depueva, A.Kh., Seismoionospheric Fountain-Effect as Analogue of Active Space Experi-

- ment, *Adv. Space Res.*, 1995, vol. 15, no. 12, pp. (12)151–(12)154.
- Ruzhin, Yu. and Depueva, A.K., Seismoprecursors in Space as Plasma and Wave Anomalies, *J. Atmos. Electr.*, 1996, vol. 16, no. 3, pp. 271–288.
- Ruzhin, Yu.Ya. and Kuznetsov, V.D., Studying Ionospheric Phenomena before Earthquakes and Other Natural and Manmade Disasters (“Volcano” Project), “*Rasprostranenie Radiovoln*”, *Sb. Dokladov 21-oi Vseross. Nauchnoi Konferentsii* (Proc. 21th All-Russia Sci. Conf. “Radiowave Propagation”), Ioshkar Ola, 2005, vol. 1, pp. 27–38.
- Ruzhin, Yu. and Larkina, V.I., Magnetic Conjugation and Time Coherency of Seismoionosphere VLF Bursts and Energetic Particles, *Proc. 13th Wroclaw EMC Symposium (URSI)*, Wroclaw, 1996, pp. 645–458.
- Ruzhin, Yu., Depueva, A.Kh., and Gorduk, V.P., Signature of Atomic Station Injection at Lower Ionosphere as Plasma Anomalies of *E* Layer, *Adv. Space Res.*, 1995, vol. 15, no. 11, pp. (11)157–(11)159.
- Sorokin, V.M., Isaev, N.V., Yaschenko, A.K., Chmyrev, V.M., and Hayakawa, M., Strong DC Electric Field Formation in the Low Latitude Ionosphere over Typhoons, *J. Atmos. Sol.–Terr. Phys.*, 2005, vol. 67, pp. 1269–1279.
- Tverskaya, L.V., Balashov, S.V., Vedenkin, N.N., Ivanov, V.V., Ivanova, T.A., Karpenko, D.S., Kochura, S.G., Maksimov, I.A., Pavlov, N.N., Rubinshtein, I.A., Tel'tsov, M.V., Trofimchuk, D.A., Tulupov, V.I., and Khartov, V.V., Solar Proton Increases and Dynamics of the Electron Outer Radiation Belt during Solar Events in December 2006, *Geomagn. Aeron.*, 2008, vol. 48, no. 6, pp. 751–758 [*Geomagn. Aeron.* (Engl. Transl.), 2008, vol. 48, pp. 719–726].